ACSNANO
www.acsnano.org
ARTICLE

Extraordinarily Bound Quasi-One-Dimensional Trions in Two-Dimensional Phosphorene Atomic Semiconductors

Renjing Xu,[†,⊥] Shuang Zhang,[†,⊥] Fan Wang,[‡] Jiong Yang,[†] Zhu Wang,[§] Jiajie Pei,[†] Ye Win Myint,[†] Bobin Xing,[†] Zongfu Yu,[§] Lan Fu,[‡] Qinghua Qin,[†] and Yuerui Lu*[,†]

[†]Research School of Engineering, College of Engineering and Computer Science, and [‡]Department of Electronic Materials Engineering, Research School of Physics and Engineering, The Australian National University, Canberra, ACT 0200, Australia
[§]Department of Electrical and Computer Engineering, University of Wisconsin, Madison, Wisconsin 53706, United States

Supporting Information

ABSTRACT: We report a trion (charged exciton) binding energy of ∼162 meV in few-layer phosphorene at room temperature, which is nearly 1−2 orders of magnitude larger than those in two-dimensional (2D) transition metal dichalcogenide semiconductors (20−30 meV) and quasi-2D quantum wells (∼1−5 meV). Such a large binding energy has only been observed in truly one-dimensional (1D) materials such as carbon nanotubes, whose optoelectronic applications have been severely hindered by their intrinsically small optical cross sections. Phosphorene offers an elegant way to overcome this hurdle by enabling quasi-1D excitonic and trionic behaviors in a large 2D area, allowing optoelectronic integration. We experimentally validated the quasi-1D nature of excitonic and trionic dynamics in phosphorene by demonstrating completely linearly polarized light emission from excitons and trions in few-layer phosphorene. The implications of the extraordinarily large trion binding energy in a higher-than-one-dimensional material are far-reaching. It provides a room-temperature 2D platform to observe the fundamental many-body interactions in the quasi-1D region.

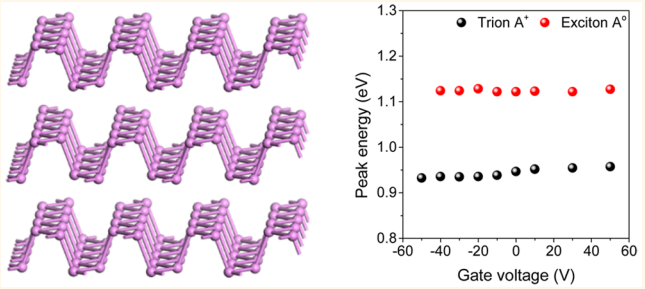

KEYWORDS: *phosphorene, trion, quasi-one-dimensional, binding energy, optoelectronic*

A neutral exciton is a bound quasi-particle state between one electron and one hole through a Coulomb interaction, similar to a neutral hydrogen atom. A trion is a charged exciton composed of two electrons and one hole (or two holes and one electron), analogous to H^- (or H_2^+).[1] Trions have been of considerable interest for the fundamental studies of many-body interactions, such as carrier multiplication and Wigner crystallization.[2] In contrast to the exciton, a trion has an extra charge with nonzero spin, which can be used for spin manipulation.[3] More importantly, the density of trions can be electrically tuned by the gate voltage, enabling remarkable optoelectronic applications.[1−5] For these purposes, a large trion binding energy is critical in order to overcome the room-temperature thermal fluctuations as well as to widen the spectral tuning range. The dimensional confinement is the dominating factor that determines the binding energy of trions. In quasi-2D quantum wells, the trion binding energy is only 1−5 meV, and trions are highly unstable, except at cryogenic temperatures.[1,6] Recently, Shan[7] and Xu[8] made an important breakthrough, showing that truly 2D atomic transition metal dichalcogenide (TMD) semiconductors have trion binding energies up to 20−30 meV, which is still barely resolvable at room temperature compared with their emission bandwidth. On the other hand, trions in the 1D space, such as carbon nanotubes, exhibit remarkably higher binding energies in the range of 100−200 meV owing to the stronger Coulomb interaction with the reduced dimensionality and screening.[9] The complete separation of the exciton and trion emission peaks was observed at room temperature.[9] However, the application of 1D carbon nanotubes for practical optoelectronic devices is intrinsically limited by their small cross sections. The overall optical responses of such 1D lines are extremely weak. The diverse distribution of the chirality in carbon nanotubes also makes it impossible to assemble a large-size film with uniform optoelectronic responses. While the reduced dimensionality leads to far more attractive exciton and trion properties, the trade-off between the cross section and the

Received: October 1, 2015
Accepted: December 29, 2015
Published: December 29, 2015

DOI: 10.1021/acsnano.5b06193
ACS Nano 2016, 10, 2046−2053

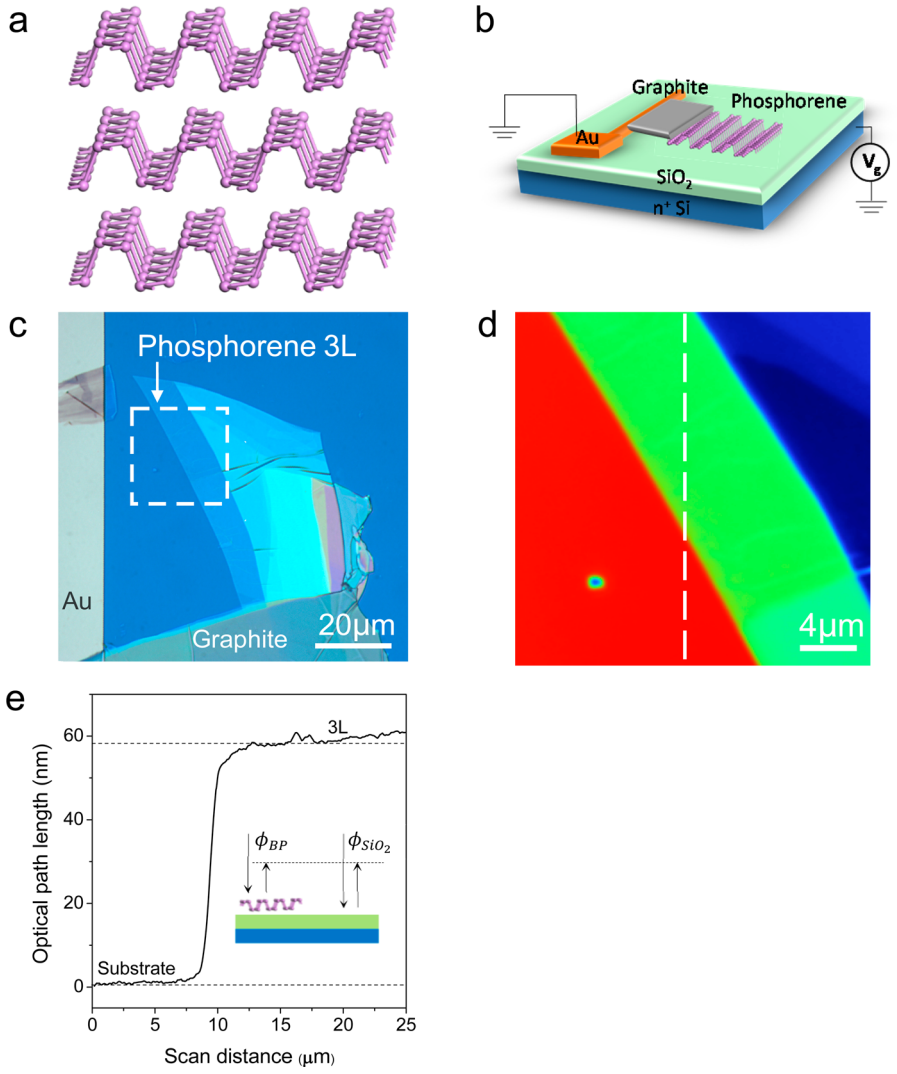

Figure 1. Phosphorene characteristics and devices. (a) Schematic plot of phosphorene layer structure. (b) Schematic plot of a phosphorene MOS device. (c) Optical microscope image of the MOS device with trilayer phosphorene (labeled as "3L"). (d) Phase-shifting interferometry image of the region inside the box indicated by the dashed line in (c). (e) PSI measured OPL values *versus* position for 3L phosphorene along the dashed line in (d). Inset: Schematic plot indicating the PSI measured phase shifts of the reflected light from the phosphorene flake (ϕ_{BP}) and the SiO_2 substrate (ϕ_{SiO_2}). The OPL is determined as $OPL_{BP} = -\lambda/2\pi(\phi_{BP} - \phi_{SiO_2})$, where λ = 535 nm is the wavelength of the light source.[42]

dimensional confinement has hindered the development of useful excitonic optoelectronic devices.

The anisotropic nature of the new 2D material phosphorene,[10−19] in contrast to other 2D materials such as graphene[20] and TMD semiconductors,[7,8,21−23] allows excitons to be confined in a quasi-one-dimensional (quasi-1D) space predicted in theory,[16,24] leading to remarkable phenomena arising from the reduced dimensionality and screening. Here, we show that phosphorene presents an intriguing platform to overcome the aforementioned trade-off. We observed quasi-1D trions with ultrahigh binding energies up to ∼162 meV in 2D phosphorene atomic semiconductors. Using back-gated metal-oxide-semiconductor (MOS) devices, we demonstrated the reversible electrostatic tunability of the exciton charging effects between trions and excitons in 3L phosphorene. The measured ultrahigh trion binding energies (∼162 meV), comparable to those in truly 1D semiconductors,[9] are due to the formation of quasi-1D trions and excitons in 2D phosphorene. The quasi-1D excitons and trions in phosphorene were demonstrated by our measured linearly polarized PL emission from the excitons and trions. In this regard, phosphorene is equivalent to a system that is made of a bundle of identical 1D materials. Our results open exciting avenues for optoelectronic applications, including tunable light sources,[4] spin manipulation devices,[3] and quantum logical systems.[5]

RESULTS AND DISCUSSION

This new type of material, few-layer phosphorene, is unstable and does not survive well in many standard nanofabrication processes.[15,25] To overcome the challenge of the instability, we designed special fabrication and characterization techniques. We used mechanical exfoliation to dry transfer[25] a phosphorene flake onto a SiO_2/Si substrate (275 nm thermal oxide on n^+-doped silicon). The phosphorene was placed near a gold electrode that was prepatterned on the substrate. Another thick graphite flake was similarly transferred to electrically bridge the phosphorene flake and the gold electrode, forming a MOS device (Figure 1). These two steps can avoid the possible

DOI: 10.1021/acsnano.5b06193
ACS Nano 2016, 10, 2046−2053

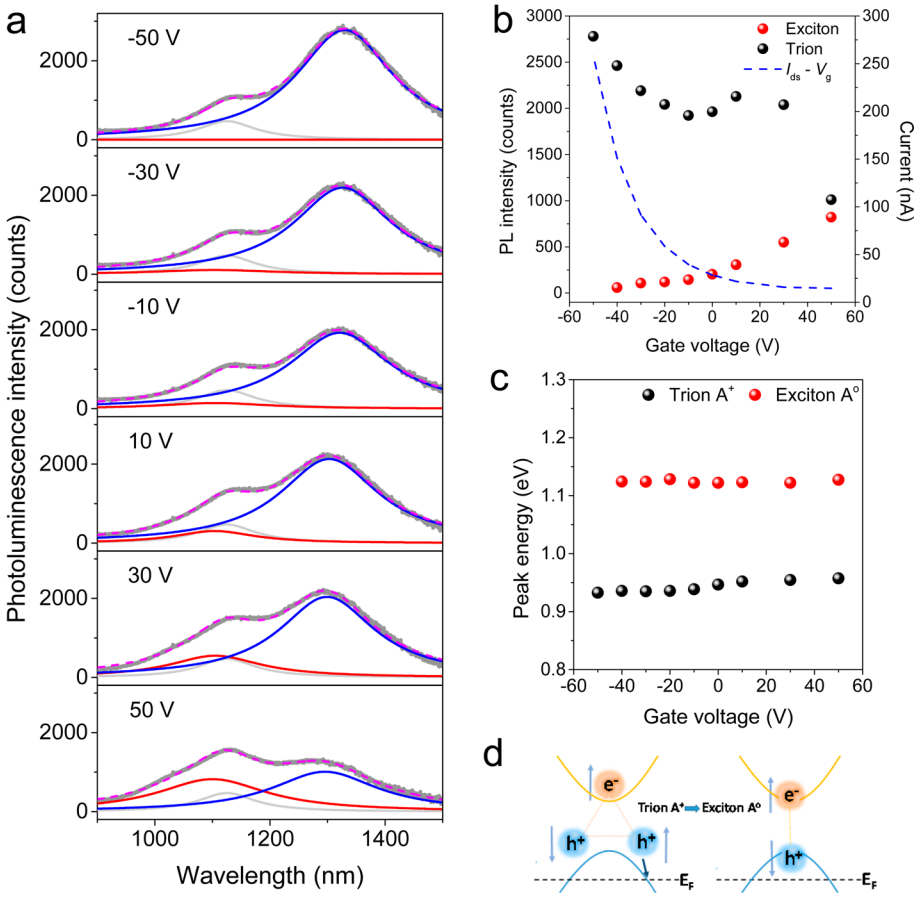

Figure 2. Gate dependence of the exciton and trion in a 3L phosphorene MOS device. (a) Measured PL spectra (solid dark gray lines) under various back-gate voltages. PL spectra are fit to Lorentzians (solid red lines are the exciton components; solid blue lines are the trion components; solid light gray lines are the Si components, and dashed pink lines are the cumulative results for the fitting). (b) PL intensity of exciton and trion (left), drain−source current as a function of gate voltages. The emergence of the charged exciton peak correlates with the onset of electrostatic doping. (c) Peak energy of exciton and trion as a function of gate voltage. (d) Schematic plot showing the dissociation of a trion into an exciton and a hole at the Fermi level.

sample cracks if we directly transfer the thin phosphorene flake onto the unflat edge of the gold electrode. This fabrication procedure kept the phosphorene free from chemical contaminations by minimizing the postprocesses after the phosphorene flake was transferred. In the measurement, the gold electrode is grounded and the n^+-doped Si substrate functions as a back gate, providing uniform electrostatic doping in the phosphorene (Figure 1b). The layer number of the phosphorene sample was precisely identified by phase-shifting interferometry (PSI), which was demonstrated by us to be a very reliable and fast way to determine the layer number for phosphorene samples.[26] After the PSI, the sample was placed into a microscope-compatible chamber for photoluminescence (PL) measurements, with a slow flow of nitrogen gas to prevent the degradation of the sample.[15] The layer number was further confirmed by the measured PL spectra.[26]

Trions, having a many-body bound state, are formed through the interplay between the exciton and carrier. The density of trions can be modulated by controlling the carrier doping level using various methods, such as electrostatic modulation[7] and chemical doping.[27] Here, we demonstrate the reversible electrostatic tunability of the exciton charging effects from positive (A^+) to neutral (A^0) in a 3L phosphorene MOS device (Figure 2), using gate-dependent PL measurements. The measured PL spectra exhibit two clear peaks with central wavelengths at ∼1100 and ∼1300 nm, whose intensities are highly dependent on the back-gate voltage. The higher-energy peak (∼1100 nm) is attributed to the exciton emission, and the lower-energy peak (∼1300 nm) is due to the trion emission.[1,7] To show the evolution of the exciton and trion, we applied a gate voltage V_g to pump extra charges into the phosphorene. We used Lorentzian curves to fit the measured PL spectra to extract the exciton and trion spectral components, as indicated by the red and blue curves in Figure 2a, respectively. The Si/SiO_2 substrate also has a PL peak at ∼1100 nm that is independent of the gate voltages (Figure S1). The emission intensity from the substrate is far weaker than that from phosphorene, and it can be easily separated from the measured voltage-dependent PL spectra (Figure 2a).

At a voltage bias of −50 V, positive charges are pumped into the phosphorene and almost all excitons become charged trions. As a result, the PL emission from neutral excitons A^0 at a wavelength of ∼1100 nm is absent (Figure 2a). In contrast, the PL emission from positive trions A^+ at ∼1300 nm is extremely strong. As we gradually depleted the positive charges by changing the voltage from −50 to 50 V, the PL emission from the neutral excitons became increasingly prominent at ∼1100 nm, while that of the positive trions became progressively weaker (Figure 2a,b) simultaneously. From the measured field-effect transistor (Figure S2) I_{ds}−V_g characteristics (Figure 2b),

DOI: 10.1021/acsnano.5b06193
ACS Nano 2016, 10, 2046−2053

we could clearly see that the emergence of the charged exciton peak correlates with the onset of electrostatic doping, which is similar to the modulation of trions in monolayer MoS_2.[7] Such a transfer of the spectral weight is directly caused by the depletion of positive charges, that is, $A^+ - h \rightarrow A^0$, where h represents a hole. In principle, negative trions can also be expected when V_g is large enough to introduce sufficient electron doping to offset the intrinsic hole doping in the phosphorene layer, which can be realized by replacing the thick oxide layer with thin, high-*k* dielectric materials. As shown in Figure 2c, the peak energy difference between excitons and trions decreased from 188 to 170 meV when the gate voltage increased from −50 to +50 V. The central wavelengths of the emission peaks from A^0 and A^+ are slightly dependent on the back-gate voltages (Figure 2c and Figure S3), which could be due to the change of Fermi level at different biases.[7,28] The peak energy difference between A^0 and A^+ exhibits a large value of ~162 meV at zero Fermi level (Figure S3), which is the trion binding energy.[8,9] Remarkably, such a large binding energy has not been observed in any other higher-than-one-dimensional material. It is comparable to that from 1D semiconductors[9,29] and is approximately 1 order of magnitude larger than that from TMD 2D semiconductors.[14,15] Positive trions with a large binding energy have been observed in multiple 3L phosphorene MOS devices (Figure S4).

In our experiments, the low-energy emission peak at ~1300 nm has opposite doping dependence with the high-energy emission peak, which agrees well with the unique behavior of trions.[7] In order to further confirm the trion assignment for the low-energy PL emission at ~1300 nm, we did excitation power-dependent PL measurements (Figure 3a). As shown by Yu *et al.*[28] and Heinz *et al.*,[30] the integrated PL intensities of localized excitons, trions/excitons, and biexcitons grow sublinearly, linearly, and quadratically, respectively, with the excitation powers.[29,31] From our measurements, the integrated PL of the low-energy peak at ~1300 nm from the 3L phosphorene sample grows linearly with the excitation power (α = 1.1, Figure 3a), indicating that the peak at ~1300 nm is indeed from trions but not from biexcitons or localized excitons, while the high-energy PL peak (~1100 nm) has been assigned to be from excitons.

Besides the electrostatic doping, substrate-induced doping can also be used to modify the spectral weight between neutral excitons and trions in the PL spectra from 2D semiconductors.[18,32] For instance, the trion emission dominates in 1L MoS_2 on the SiO_2 substrate, while the neutral exciton emission dominates in 1L MoS_2 on the gold substrate since 1L MoS_2 has an initial n-type doping and the gold substrate can reduce the doping level *via* charge transfer between the gold–MoS_2 interface.[31] Although the tunability of the excitons and trions through the electrical gate is obvious in Figure 2a, the exciton emission peak at ~1100 nm from 3L phosphorene partially overlaps with the PL emission of the silicon substrate. In order to get rid of the PL influence from the silicon substrate and see the exciton emission of 3L phosphorene more clearly, we transferred a 3L phosphorene sample onto a gold substrate. Interestingly, the unambiguous exciton emission peak at ~1080 nm was observed from the 3L phosphorene on gold (Figure 3b), in contrast to the dominant trion emission peak at ~1300 nm from 3L phosphorene on the SiO_2 substrate. This strongly substrate-dependent PL response can be understood from the charge transfer between the 3L phosphorene and the gold substrate, as indicated in the schematic plot of the band

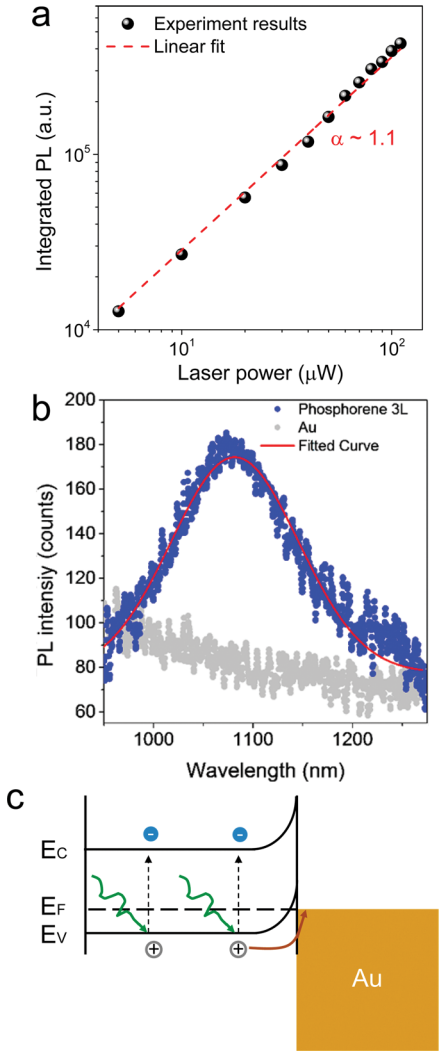

Figure 3. Power dependence of trion emission and substrate-induced PL modification in a 3L phosphorene. (a) Measured integrated PL intensity of the trion emission (~1300 nm), from a 3L phosphorene sample on a SiO_2/Si substrate, as a function of the applied laser power. The dashed line represents the power-law fit, with exponent of α = 1.1. (b) Measured PL spectra from a 3L phosphorene on a gold substrate and PL spectra from the gold substrate as background comparison. The gold substrate is not grounded during the experiment. (c) Schematic plot of the energy band diagram for the 3L phosphorene–gold hybrid system, showing the charge transfer and the quenching effect during the PL process.

diagram[32] (Figure 3c). During the PL measurements, the excited holes will move toward the gold surface and then annihilate with the electrons from gold, which can significantly reduce the doping level (from the initial p-type dopants) in 3L phosphorene and make the PL emission from neutral excitons dominant. This charge transfer can also quench the intensity of the PL emission. That is why the PL intensity from the 3L phosphorene on gold is relatively low, which is similar to that from 1L MoS_2 on gold.[31] Owing to the significant reduction of the doping level and the quenching effect, the trion peak at ~1300 nm was not observed from the 3L phosphorene on the gold substrate.

The ultrahigh trion binding energy measured in few-layer phosphorene is caused by the material's unique anisotropic

DOI: 10.1021/acsnano.5b06193
ACS Nano 2016, 10, 2046–2053

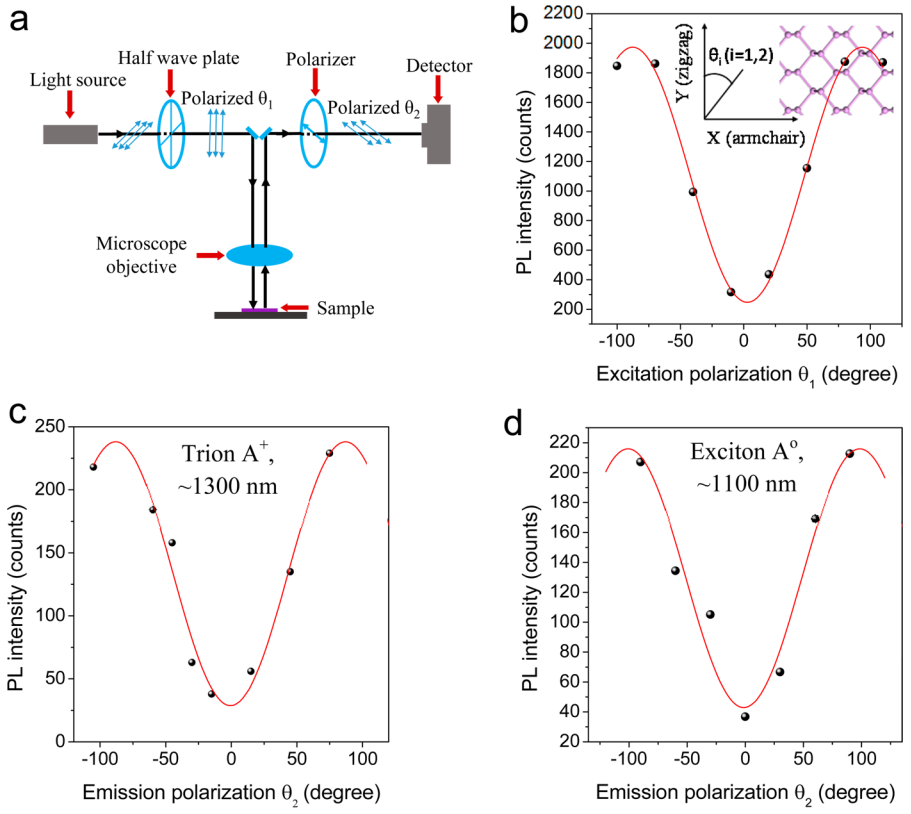

Figure 4. Quasi-1D trions and excitons in 3L phosphorene. (a) Schematic plot of the setup for measurement to characterize the polarization dependence of PL excitation and emission. The polarization angle (θ_1) incident excitation light is controlled by an angle-variable half-wave plate, and the polarization angle (θ_2) of the PL emission is characterized by inserting an angle-variable polarizer in front of the detector. (b) Measured excitation polarization dependence of the trion emission (~1300 nm) peak intensities from a 3L phosphorene on the SiO_2/Si substrate. For this measurement, the polarizer in front of the detector was removed. Inset: Schematic plot showing top view of the phosphorene lattice structure and coordinates for polarization angles θ_1 and θ_2. (c,d) Measured polarization dependence of the trion (A^+) emission at ~1300 nm (c) and the exciton (A^0) emission at ~1100 nm (d), measured from a 3L phosphorene on SiO_2/Si, with a fixed excitation angle of 95°.

quasi-1D excitonic nature, which can be measured using the linearly polarized emission, as theoretically predicted by Yang *et al.*[16] Here, we demonstrate the quasi-1D nature of the excitons and trions in few-layer phosphorene using PL measurements with an angle-resolved excitation and emission. We show that the PL emissions are completely linearly polarized along the armchair direction of the crystal. In the setup of the angle-resolved PL measurement (Figure 4a), a linearly polarized Nd:YAG laser with a wavelength of 532 nm was used as the excitation source. The polarization angle of the incident light (θ_1) is controlled by an angle-variable half-wave plate. The polarization angle of the emission (θ_2) is characterized by inserting an angle-variable polarizer in front of the detector. θ_1 and θ_2 are relative to the same zero-degree reference, which can be arbitrarily selected in the beginning. According to the polarization-dependent PL excitation, we can determine the crystalline orientation of the phosphorene flake, and then the zigzag direction is selected as the shared zero-degree reference for θ_1 and θ_2 (Figure 4b inset). In the first characterization of the PL excitation polarization dependence, only the half-wave plate was used, and the polarizer in front of the detector was removed. We found that the PL intensity strongly depends on the excitation polarization angle θ_1 (Figure 4b and Figure S5). This strong PL excitation polarization dependence is due to the highly anisotropic optical absorption in the phosphorene.[16] Because of the symmetry in its band structure and the optical selection rules,[24,33] phosphorene strongly absorbs armchair-polarized light and is transparent to zigzag-polarized light with energies between 0.5 and 2.8 eV.[16] Next, we measured the polarization of the PL emission by fixing the excitation polarization angle θ_1. We observed the maximum PL intensity at θ_2 = 90° and the minimum PL intensity at θ_2 = 0° (Figure 4c,d). From Figure 4c,d, we could clearly see that the PL emissions from both trions (~1300 nm) and excitons (~1100 nm) in the 3L phosphorene are completely linearly polarized along the armchair direction. The measured linear dichroism (LD) values for the PL emissions are all close to unity in few-layer phosphorene samples (Figure 4c,d). LD is defined as LD = $(I_x - I_y)/I_x$, where I_x and I_y are the PL emission peak intensities along the armchair and zigzag directions, respectively. The polarization of the PL emission is independent of the excitation and is determined by the intrinsic properties of phosphorene.[33]

To better understand the extraordinary trion binding energy (as large as ~162 meV) for 3L phosphorene, a theoretical analysis is important. Until now, exciton and trion binding energies have been calculated using many different well-developed approaches, such as diffusion Monte Carlo technique,[34,35] the boundary-matching-matrix method,[36] and hyperspherical approach,[37,38] *etc.* However, they are mainly applicable for 2D TMD semiconductors and quasi-2D GaAs quantum wells.[34−38] We tried to implement these approaches

DOI: 10.1021/acsnano.5b06193
ACS Nano 2016, 10, 2046−2053

for 3L phosphorene and obtained the trion binding energy of 50−70 meV,[34−38] which is lower than the value measured from our experiments. This is primarily because the excitons and trions in phosphorene are confined to a quasi-1D space, which has been demonstrated by our angle-resolved PL measurements on 3L phosphorene samples. Here, we calculate the quasi-1D trion binding energy using a variational quantum Monte Carlo method because this approach has been demonstrated to work well for both quasi-1D trions from carbon nanotubes and quasi-2D trions from GaAs quantum wells.[9,30,40−42] The binding energies of excitons (E_E) and trions (E_T) can be estimated using the following equation:[39]

$$E_E = \frac{4}{(D_E - 1)^2} \times R_y^*$$

$$E_T = \left(-\frac{4}{(D_E - 1)^2} - c_0 - \sum_{i=1}^{4} c_i D_T^{-i} e^{-D_T} \right) \times R_y^* \quad (1)$$

where D_E is the effective dimension of excitons, D_T is the effective dimension of trions, R_y^* is the effective Rydberg, and $c_{i,i=1-4}$ are coefficients[39] given in Supporting Information Table S1.

The effective dimension of a trion is expected to be slightly smaller than that of an exciton because of the extra charge in the trion.[39] For calculation and analysis convenience,[39] we can simply the equation by taking $D = D_E = D_T$.

$$E_E = \frac{4}{(D - 1)^2} \times R_y^*$$

$$E_T = \left(-\frac{4}{(D - 1)^2} - c_0 - \sum_{i=1}^{4} c_i D^{-i} e^{-D} \right) \times R_y^* \quad (2)$$

The calculated trion binding using this simplified eq 2 is expected to be slightly smaller than that from the original eq 1. Based on this simplified eq 2, we calculated the trion and exciton binding energies as a function of the effective dimension D in 3L phosphorene (Figure S6). Using the measured trion binding energy value of ∼162 meV in 3L phosphorene, we can estimate the effective dimension of trions in 3L phosphorene to be $D \sim 1.58$, which further supports the quasi-1D nature of trions demonstrated earlier. Based on previous theoretical calculations, the trion binding energies of TMDs materials are 10−15% of their exciton binding energies,[34−38] and this has been confirmed by experimental measurements in TMD semiconductors.[7,8,23] Based on Tran's simulation,[16] the exciton binding energy of monolayer phosphorene (∼0.9 eV) is higher than the exciton binding energies of all reported TMD monolayers,[34−38,40,41] because of the quasi-1D exciton nature in phosphorene.[16] More importantly, based on eq 2 and Figure S6, the binding energies of excitons and trions increase with the decrease of the effective dimensionality of the exitons and trions in the materials. This is the main reason that trions in the 1D space, such as carbon nanotubes, own remarkably higher binding energies in the range of ∼200 meV.[9]

CONCLUSIONS

In conclusion, we observed extraordinarily bound quasi-1D trions in 2D phosphorene atomic semiconductor crystals. The measured ultrahigh trion binding energies in few-layer phosphorene are approximately 1 order of magnitude higher than those in 2D TMD semiconductors. The large trion binding energy is due to the strongly confined quasi-1D excitonic nature in few-layer phosphorene, which is demonstrated by our measured linearly polarized PL emission. Phosphorene possesses both a large optical cross section, as typically exhibited by a 2D material system, and high trion binding energies, as typically exhibited by a 1D system, allowing remarkable optoelectronic applications, including tunable light sources, photodetectors, and spin manipulation devices. Few-layer phosphorene also serves as a room-temperature platform for investigating many-body interactions and excitonic physics.

EXPERIMENTAL METHODS

Device Fabrication and Characterization. We used mechanical exfoliation to dry transfer[25] a phosphorene flake onto a SiO_2/Si substrate (275 nm thermal oxide on n^+-doped silicon), near a prepatterned gold electrode. The gold electrodes were patterned by conventional photolithography, metal deposition, and lift-off processes. Another thick graphite flake was similarly transferred to electrically bridge the phosphorene flake and the gold electrode, forming a MOS device. All PL and polarization measurements were conducted using a T64000 micro-Raman system equipped with a charge-coupled device and InGaAs detectors, along with a 532 nm Nd:YAG laser as the excitation source. Subsequent to PSI measurement, the sample was placed into a Linkam THMS 600 chamber, with a slow flow of nitrogen gas to prevent degradation of the sample.[15] To avoid laser-induced sample damage, all PL spectra were recorded at low power levels: $P \sim 20$ μW. For the PL measurements, an integration time of 30 s was used. The electrical bias was applied using a Keithley 4200 semiconductor analyzer.

Numerical Simulation. Stanford Stratified Structure Solver (S4) was used to calculate the phase delay. The method numerically solves Maxwell's equations in multiple layers of structured materials by expanding the field in the Fourier space.

ASSOCIATED CONTENT

Supporting Information

The Supporting Information is available free of charge on the ACS Publications website at DOI: 10.1021/acsnano.5b06193.

Details of more experimental PL measurement results and data analysis (PDF)

AUTHOR INFORMATION

Corresponding Author

*E-mail: yuerui.lu@anu.edu.au.

Author Contributions

⊥R.X. and S.Z. contributed equally to this work.

Author Contributions

Y.R.L. designed the project; S.Z. did the PL and Raman measurements and data analysis; R.J.X. conducted the device fabrication, PL data fitting analysis, and part of the theoretical calculations; S.Z. and R.J.X. conducted the PSI measurements; J.Y., J.J.P., and Y.W.M. contributed to sample preparation; B.B.X. performed the image postprocessing; F.W. and L.F. built the optical characterization setup; Z.W. and Z.F.Y. performed the theoretical simulations for the OPL of phosphorene. All authors contributed to the manuscript.

Notes

The authors declare no competing financial interest.

ACKNOWLEDGMENTS

We acknowledge support from the ACT node of the Australian National Fabrication Facility (ANFF). We also thank Professor

DOI: 10.1021/acsnano.5b06193
ACS Nano 2016, 10, 2046−2053

Chennupati Jagadish, Professor Hoe Tan, and Professor Barry Luther-Davies from the Australian National University for facility support, as well as Dr. Gang Zhang from the Institute of High Performance Computing, A*STAR, Singapore, for the helpful discussions. We acknowledge financial support from an ANU Ph.D. scholarship, the Office of Naval Research (USA) (Grant No. N00014-14-1-0300), the Australian Research Council (Grant No. DE140100805), and the ANU Major Equipment Committee (Grant No. 14MEC34).

REFERENCES

(1) Kheng, K.; Cox, R. T.; d'Aubigné, M. Y.; Bassani, F.; Saminadayar, K.; Tatarenko, S. Observation of Negatively Charged Excitons in Semiconductor Quantum Wells. *Phys. Rev. Lett.* **1993**, *71*, 1752−1755.

(2) Wigner, E. On the Interaction of Electrons in Metals. *Phys. Rev.* **1934**, *46*, 1002−1011.

(3) Xu, X.; Yao, W.; Xiao, D.; Heinz, T. F. Spin and Pseudospins in Layered Transition Metal Dichalcogenides. *Nat. Phys.* **2014**, *10*, 343−350.

(4) Scholes, G. D.; Rumbles, G. Excitons in Nanoscale Systems. *Nat. Mater.* **2006**, *5*, 683−696.

(5) High, A. A.; Novitskaya, E. E.; Butov, L. V.; Hanson, M.; Gossard, A. C. Control of Exciton Fluxes in an Excitonic Integrated Circuit. *Science* **2008**, *321*, 229−231.

(6) Huard, V.; Cox, R. T.; Saminadayar, K.; Arnoult, A.; Tatarenko, S. Bound States in Optical Absorption of Semiconductor Quantum Wells Containing a Two-Dimensional Electron Gas. *Phys. Rev. Lett.* **2000**, *84*, 187−190.

(7) Mak, K. F.; He, K.; Lee, C.; Lee, G. H.; Hone, J.; Heinz, T. F.; Shan, J. Tightly Bound Trions in Monolayer MoS_2. *Nat. Mater.* **2013**, *12*, 207−211.

(8) Ross, J. S.; Wu, S.; Yu, H.; Ghimire, N. J.; Jones, A. M.; Aivazian, G.; Yan, J.; Mandrus, D. G.; Xiao, D.; Yao, W.; Xu, X. Electrical Control of Neutral and Charged Excitons in a Monolayer Semiconductor. *Nat. Commun.* **2013**, *4*, 1474.

(9) Matsunaga, R.; Matsuda, K.; Kanemitsu, Y. Observation of Charged Excitons in Hole-Doped Carbon Nanotubes Using Photoluminescence and Absorption Spectroscopy. *Phys. Rev. Lett.* **2011**, *106*, 037404.

(10) Liu, H.; Neal, A. T.; Zhu, Z.; Luo, Z.; Xu, X.; Tománek, D.; Ye, P. D. Phosphorene: An Unexplored 2D Semiconductor with a High Hole Mobility. *ACS Nano* **2014**, *8*, 4033−4041.

(11) Buscema, M.; Groenendijk, D. J.; Blanter, S. I.; Steele, G. A.; van der Zant, H. S. J.; Castellanos-Gomez, A. Fast and Broadband Photoresponse of Few-Layer Black Phosphorus Field-Effect Transistors. *Nano Lett.* **2014**, *14*, 3347−3352.

(12) Fei, R.; Yang, L. Strain-Engineering the Anisotropic Electrical Conductance of Few-Layer Black Phosphorus. *Nano Lett.* **2014**, *14*, 2884−2889.

(13) Xia, F.; Wang, H.; Jia, Y. Rediscovering Black Phosphorus as an Anisotropic Layered Material for Optoelectronics and Electronics. *Nat. Commun.* **2014**, *5*, 4458.

(14) Li, L.; Yu, Y.; Ye, G. J.; Ge, Q.; Ou, X.; Wu, H.; Feng, D.; Chen, X. H.; Zhang, Y. Black Phosphorus Field-Effect Transistors. *Nat. Nanotechnol.* **2014**, *9*, 372−377.

(15) Zhang, S.; Yang, J.; Xu, R.; Wang, F.; Li, W.; Ghufran, M.; Zhang, Y.-W.; Yu, Z.; Zhang, G.; Qin, Q.; Lu, Y. Extraordinary Photoluminescence and Strong Temperature/Angle-Dependent Raman Responses in Few-Layer Phosphorene. *ACS Nano* **2014**, *8*, 9590−9596.

(16) Tran, V.; Soklaski, R.; Liang, Y.; Yang, L. Layer-Controlled Band Gap and Anisotropic Excitons in Few-Layer Black Phosphorus. *Phys. Rev. B: Condens. Matter Mater. Phys.* **2014**, *89*, 235319.

(17) Hong, T.; Chamlagain, B.; Lin, W.; Chuang, H.-J.; Pan, M.; Zhou, Z.; Xu, Y.-Q. Polarized Photocurrent Response in Black Phosphorus Field-Effect Transistors. *Nanoscale* **2014**, *6*, 8978−8983.

(18) Tongay, S.; Suh, J.; Ataca, C.; Fan, W.; Luce, A.; Kang, J. S.; Liu, J.; Ko, C.; Raghunathanan, R.; Zhou, J.; Ogletree, F.; Li, J.; Grossman, J. C.; Wu, J. Defects Activated Photoluminescence in Two-Dimensional Semiconductors: Interplay between Bound, Charged, and Free Excitons. *Sci. Rep.* **2013**, *3*, 2657.

(19) Xu, R.; Yang, J.; Zhu, Y.; Yan, H.; Pei, J.; Myint, Y. W.; Zhang, S.; Lu, Y. Layer-Dependent Surface Potential of Phosphorene and Anisotropic/Layer-Dependent Charge Transfer in Phosphorene-Gold Hybrid Systems. *Nanoscale* **2016**, *8*, 129.

(20) Geim, A. K.; Novoselov, K. S. The Rise of Graphene. *Nat. Mater.* **2007**, *6*, 183−191.

(21) Yang, J.; Lü, T.; Myint, Y. W.; Pei, J.; Macdonald, D.; Zheng, J.-C.; Lu, Y. Robust Excitons and Trions in Monolayer $MoTe_2$. *ACS Nano* **2015**, *9*, 6603−6609.

(22) Yang, J.; Wang, Z.; Wang, F.; Xu, R.; Tao, J.; Zhang, S.; Qin, Q.; Luther-Davies, B.; Jagadish, C.; Yu, Z.; Lu, Y. Atomically Thin Optical Lenses and Gratings. *arXiv:1411.6200* **2014**.

(23) Pei, J.; Yang, J.; Xu, R.; Zeng, Y.-H.; Myint, Y. W.; Zhang, S.; Zheng, J.-C.; Qin, Q.; Wang, X.; Jiang, W.; Lu, Y. Exciton and Trion Dynamics in Bilayer MoS_2. *Small* **2015**, *11*, 6384.

(24) Qiao, J.; Kong, X.; Hu, Z.-X.; Yang, F.; Ji, W. High-Mobility Transport Anisotropy and Linear Dichroism in Few-Layer Black Phosphorus. *Nat. Commun.* **2014**, *5*, 4475.

(25) Castellanos-Gomez, A.; Buscema, M.; Molenaar, R.; Singh, V.; Janssen, L.; van der Zant, H. S. J.; Steele, G. A. Deterministic Transfer of Two-Dimensional Materials by All-Dry Viscoelastic Stamping. *2D Mater.* **2014**, *1*, 011002.

(26) Yang, J.; Xu, R.; Pei, J.; Myint, Y. W.; Wang, F.; Wang, Z.; Zhang, S.; Yu, Z.; Lu, Y. Optical Tuning of Exciton and Trion Emissions in Monolayer Phosphorene. *Light: Sci. Appl.* **2015**, *4*, e312.

(27) Mouri, S.; Miyauchi, Y.; Matsuda, K. Tunable Photoluminescence of Monolayer Mos2 *via* Chemical Doping. *Nano Lett.* **2013**, *13*, 5944−5948.

(28) Shang, J.; Shen, X.; Cong, C.; Peimyoo, N.; Cao, B.; Eginligil, M.; Yu, T. Observation of Excitonic Fine Structure in a 2D Transition-Metal Dichalcogenide Semiconductor. *ACS Nano* **2015**, *9*, 647−655.

(29) Park, J. S.; Hirana, Y.; Mouri, S.; Miyauchi, Y.; Nakashima, N.; Matsuda, K. Observation of Negative and Positive Trions in the Electrochemically Carrier-Doped Single-Walled Carbon Nanotubes. *J. Am. Chem. Soc.* **2012**, *134*, 14461−14466.

(30) You, Y.; Zhang, X.-X.; Berkelbach, T. C.; Hybertsen, M. S.; Reichman, D. R.; Heinz, T. F. Observation of Biexcitons in Monolayer Wse2. *Nat. Phys.* **2015**, *11*, 477−481.

(31) Buscema, M.; Steele, G.; van der Zant, H. J.; Castellanos-Gomez, A. The Effect of the Substrate on the Raman and Photoluminescence Emission of Single-Layer MoS_2. *Nano Res.* **2014**, *7*, 561−571.

(32) Cai, Y.; Zhang, G.; Zhang, Y.-W. Layer-Dependent Band Alignment and Work Function of Few-Layer Phosphorene. *Sci. Rep.* **2014**, *4*, 6677.

(33) Yuan, H.; Liu, X.; Afshinmanesh, F.; Li, W.; Xu, G.; Sun, J.; Lian, B.; Ye, G.; Hikita, Y.; Shen, Z.; Zhang, S.-C.; Chen, X.; Brongersma, M.; Hwang, H. Y.; Cui, Y. Broadband Linear-Dichroic Photodetector in a Black Phosphorus Vertical P-N Junction. *arXiv:1409.4729* **2014**.

(34) Ceperley, D. M.; Alder, B. Ground State of the Electron Gas by a Stochastic Method. *Phys. Rev. Lett.* **1980**, *45*, 566.

(35) Needs, R.; Towler, M.; Drummond, N.; Lopez Ríos, P. Continuum Variational and Diffusion Quantum Monte Carlo Calculations. *J. Phys.: Condens. Matter* **2010**, *22*, 023201.

(36) Ganchev, B.; Drummond, N.; Aleiner, I.; Fal'ko, V. Three-Particle Complexes in Two-Dimensional Semiconductors. *Phys. Rev. Lett.* **2015**, *114*, 107401.

(37) Thilagam, A. Exciton Complexes in Low Dimensional Transition Metal Dichalcogenides. *J. Appl. Phys.* **2014**, *116*, 053523.

(38) Ruan, W.; Chan, K.; Ho, H.; Zhang, R.; Pun, E. Hyperspherical Approach for Charged Excitons in Quantum Wells. *Phys. Rev. B: Condens. Matter Mater. Phys.* **1999**, *60*, 5714.

(39) Rønnow, T. F.; Pedersen, T. G.; Partoens, B.; Berthelsen, K. K. Variational Quantum Monte Carlo Study of Charged Excitons in

DOI: 10.1021/acsnano.5b06193
ACS Nano 2016, 10, 2046−2053

Fractional Dimensional Space. *Phys. Rev. B: Condens. Matter Mater. Phys.* **2011**, *84*, 035316.
(40) Ugeda, M. M.; Bradley, A. J.; Shi, S.-F.; da Jornada, F. H.; Zhang, Y.; Qiu, D. Y.; Ruan, W.; Mo, S.-K.; Hussain, Z.; Shen, Z.-X.; Wang, F.; Louie, S. G.; Crommie, M. F. Giant Bandgap Renormalization and Excitonic Effects in a Monolayer Transition Metal Dichalcogenide Semiconductor. *Nat. Mater.* **2014**, *13*, 1091−1095.
(41) Ye, Z.; Cao, T.; O'Brien, K.; Zhu, H.; Yin, X.; Wang, Y.; Louie, S. G.; Zhang, X. Probing Excitonic Dark States in Single-Layer Tungsten Disulphide. *Nature* **2014**, *513*, 214−218.
(42) Yang, J.; Xu, R.; Pei, J.; Myint, Y. W.; Wang, F.; Wang, Z.; Zhang, S.; Yu, Z.; Lu, Y. Unambiguous Identification of Monolayer Phosphorene by Phase-Shifting Interferometry. *arXiv:1412.6701* **2014**.

DOI: 10.1021/acsnano.5b06193
ACS Nano 2016, 10, 2046−2053